



# The effect of Co substitution for Cu in $\text{Bi}_2\text{Sr}_2\text{Ca}_1\text{Cu}_2\text{O}_{8-\delta}$

Y.-K. Kuo<sup>a</sup>, C.W. Schneider<sup>a</sup>, D.T. Verebelyi<sup>a</sup>, M.V. Nevitt<sup>a</sup>, M.J. Skove<sup>a,\*</sup>,  
G.X. Tessema<sup>a</sup>, He Li<sup>b</sup>, J.M. Pond<sup>c</sup>

<sup>a</sup> Department of Physics and Astronomy, Clemson University, Clemson, SC 29634-1911, USA

<sup>b</sup> Department of Chemistry, Clemson University, Clemson, SC 29634-1905, USA

<sup>c</sup> Naval Research Laboratory, Washington, DC 20375-5000, USA

Received 14 July 1998; received in revised form 6 January 1999; accepted 5 April 1999

## Abstract

We have grown single crystal whiskers of  $\text{Bi}_2(\text{SrCa})_{n+1}(\text{Cu}_{1-x}\text{Co}_x)_n\text{O}_{8-\delta}$  with  $0 < x < 0.26$ , and measured their resistance  $R$  as a function of the temperature  $T$ . For  $x < 0.06$ ,  $n = 2$  in the majority of the sample and  $n = 3$  in a small part. For both phases, the changes in  $T_c$  and in the extrapolated residual resistance due to Co substitution are the same for Co as it is for Zn and Ni, indicating that magnetic scattering is not important. For  $x \approx 0.06$ , oxygenation can drive the sample from superconducting to insulating, indicating that both the scattering of the carriers and the number of carriers affect the superconducting–insulating transition. This occurs in samples in which the sheet resistance in a CuO plane is approximately  $h/(2e)^2$ . For  $x > 0.18$ , the samples are insulating and  $n = 1$ . © 1999 Elsevier Science B.V. All rights reserved.

**Keywords:** Metal–insulator transition; Whiskers; Pair-breaking

## 1. Introduction

It is well established that the cuprate high- $T_c$  superconductors are close to the insulating phase, and can be driven through the transition by changes in carrier concentration and/or by impurities that increase the scattering of the carriers in the copper oxide planes [1]. The superconducting–insulating transition (SIT) is important in understanding both the normal and superconducting states of the cuprates.

One thought is that the SIT is driven by changing the carrier concentration [1]. This can be done either by impurity substitution or oxygen doping. For ex-

ample, it has been shown that substituting rare-earth trivalent ions for  $\text{Ca}^{2+}$  ions drives superconducting  $\text{Bi}_2\text{Sr}_2\text{CaCu}_2\text{O}_{8+\delta}$  (Bi-2212) system through an SIT [2–4]. Similar transitions were also observed in the other cuprates  $\text{La}_{2-x}\text{Sr}_x\text{CuO}_4$  (214) and  $\text{YBa}_2\text{Cu}_3\text{O}_{7-y}$  (123) with a critical hole-doping concentration of about  $x_c = 0.05$  for 214 and  $y_c = 0.5$  for 123 [5–7]. It is generally agreed that  $\text{La}_2\text{CuO}_4$  and  $\text{YBa}_2\text{Cu}_3\text{O}_6$  are correlation-dominated Mott–Hubbard insulators, while the overdoped metallic side is essentially Fermi-liquid like. An inverted U dependence of the superconducting transition temperature,  $T_c$ , on carrier concentration has been generally observed in the cuprates [8].

On the other hand there are studies in films of elemental superconductors [9], as well as in the

\* Corresponding author. Tel.: +1-864-656-3416; Fax: +1-864-656-0805.

cuprates, which concentrate on the localization of electrons by scattering from impurities, surfaces or other defects. Different parent materials, growth techniques, substituents and approaches (starting from the insulating or superconducting phase) have been reported [10–17]. Usually no metallic ground state between insulating and superconducting phases was found, (i.e.,  $\lim_{T \rightarrow 0} \rho$  is either 0 or  $\infty$ ). At low doping levels, the low temperature behavior of the resistivity  $\rho$  in the insulating phase can be fit reasonably well to the hopping conduction form  $\rho(T) = \rho_0 \exp(T_0/T)^\eta$ . Different values of the exponent  $\eta$  have been reported, with  $\eta = 1/4$  (three-dimensional variable range hopping (VRH) of localized states) [16,18],  $\eta = 1/3$  (two-dimensional VRH) [19],  $\eta = 1/2$  (VRH in the presence of a Coulomb gap) [5,13] or even an  $\eta$  dependent on doping concentration [11].

In the Bi-2212 system, most of the SIT studies have been done by substituting rare earth ions for Ca ions in sintered polycrystalline samples, because material composition can be controlled rather precisely and large samples are available [19,20]. The critical concentration for the SIT was found to be about 50% substitution for Ca and independent of substituent. The nature of the SIT is usually attributed to single-particle localization as a result of introducing disorder [10,12,19], or the opening of a mobility edge in the vicinity of the Fermi level [13]. Another approach to this problem is to substitute on the Cu sites. There is a fundamental difference between substitution on the Cu sites and on the Ca sites in Bi-2212. The effect of substitution on the Cu sites is much stronger than on Ca sites (or oxygen doping) since the former affects the superconducting properties directly through the changes in copper oxide planes, while the latter mainly affects the charge reservoir, although the carriers may suffer some scattering by the substitutions for the nearby Ca. Several studies showed that the depression of  $T_c$  obtained by substituting on the Cu sites in Bi-2212 is the result of pair-breaking processes in the CuO planes [21]. However, the lowering of  $T_c$  due to unbinding of Cooper pairs would be expected to lead to a superconductor–metal transition as opposed to the SIT commonly observed in this material [22]. Alternatively, carrier localization induced by disorder, enhanced by the strongly two-dimensional char-

acter of BiSCCO, has become more attractive in explaining the depression of  $T_c$  and the SIT [10,12].

Studies have been reported on 3d transition metal substitutions in  $\text{Bi}_2\text{Sr}_2\text{Ca}(\text{Cu}_{1-x}\text{M}_x)_2\text{O}_{8+\delta}$  polycrystals [23–26] and single crystals ( $T_c \sim 80$  K) [12,14,21,27–29]. The single crystal work generally shows a similar depression rate of  $T_c$  ( $dT_c/dx \approx -800$  K), independent of the substitutional element. The theory of Radtke et al. [30] predicts that  $dT_c/dx$  should indeed depend only on the residual resistance. However, the SIT driven by Cu site substitution has rarely been studied on single crystals. This is due to the restricted limits for Cu replacement that have been observed in single crystal growth, which often prevents reaching the insulating side in this system. It has been reported that the limits for replacement are reached at about  $x = 0.02$  for Ni and  $x = 0.004$  for Zn by the directional solidification technique [21], and  $x = 0.016$  for Co and  $x = 0.03$  for Ni by the self-flux technique [12]. All those samples studied were still in the superconducting phase, although a minimum in  $R$  vs.  $T$  near  $T_c$  was observed in an  $x = 0.016$  Co substituted Bi-2212 single crystal [12]. A study of self-flux-grown, Co substituted, single crystals in multi-phase aggregates showed a limit of  $x = 0.08$  Co in the 2212 phase and an insulating 2201 phase for  $x > 0.08$  [29].

We have previously reported the effect of Ni and Zn substitution for Cu in BiSCCO whiskers in which we found that the solubility limits are about  $x = 0.018$  for Ni and  $x = 0.007$  for Zn [27], consistent with the observation of vom Hede et al. [21] on larger single crystals. In this work, we present the effect of substitution in  $\text{Bi}_2(\text{SrCa})_{n+1}(\text{Cu}_{1-x}\text{Co}_x)_n\text{O}_y$  whiskers containing both the 2212 and 2223 phase (for lower  $x$ ), and whiskers containing the (2201) phase (for higher  $x$ ). Following earlier work, we make the essential assumption that the compositional substitution of Co for Cu corresponds to a one-for-one replacement of Cu atoms by Co atoms in the Cu–O layers. While we lack experimental evidence for this in BiSCCO crystals, X-ray and neutron scattering [31–33], as well as XAFS measurements [34] show that Cu-site substitution by the 3d transition metals Fe, Co and Ni occurs in the Cu–O planes of YBCO. We believe that general chemical considerations support our making this assumption for BiSCCO. The much higher solubility limit for Co in our whisker

crystals, grown by a different technique, allows us to study the SIT in very fine detail. The effect of oxygen doping was also examined at several levels of Co substitution.

## 2. Experimental details

### 2.1. Crystal preparation and compositional analysis

The BiSCCO whiskers were grown by the method pioneered by Matsubara et al. [35]. The proper ratio of starting materials from oxides and carbonates with desired amounts of CoO were mixed, melted at 1250°C, splat-cooled, and whiskers produced by placing the resultant glass shards in flowing oxygen at one atmosphere at about 850°C for at least 120 h. Typical dimensions of the whiskers are 2–10 mm (*a*-axis), 10–100 μm (*b*-axis) and 2–10 μm (*c*-axis). Sample dimensions diminish considerably as more Co is substituted for Cu in the starting materials. The oxygen content of the whiskers was adjusted by annealing them at 580°C in various partial pressures of O<sub>2</sub>, such as zero (Ar annealed), 0.2 atm (air), 1 atm and 2 atm.

Quantitative compositional analysis of substituted samples was done by non-destructive electron probe microanalysis techniques using a Cameca SX50 four-wavelength spectrometer automated electron microprobe. The minimum limits of detection, based on the standard peak and background counts and the stated counting times are ~0.025% for Co. As oxide components, the stated detection limits are ~0.034% for CoO. The detailed error analysis of our composition determination is reported elsewhere [27]. We found the composition to be uniform within 5% (for each constituent) along the sample length. We can substitute Co for Cu in the glass up to  $x_{\text{init}} \approx 0.15$  (where  $x_{\text{init}}$  is Co/(Cu + Co) in the glass), from which whiskers with Co concentrations up to  $x = 0.26$  grow. In Fig. 1 we plot the chemical composition in the whiskers measured by microprobe vs.  $x_{\text{init}}$ . Note that high quality BiSCCO single crystals (as judged from the width of the superconducting transition) do not have a stoichiometry ratio of exactly 2212. For example, Lombardo and Kapit-ulnik [36] find Bi<sub>2.12</sub>(Sr<sub>1-x</sub>Ca<sub>x</sub>)<sub>2.83</sub>Cu<sub>2.05</sub>O<sub>8+δ</sub>,

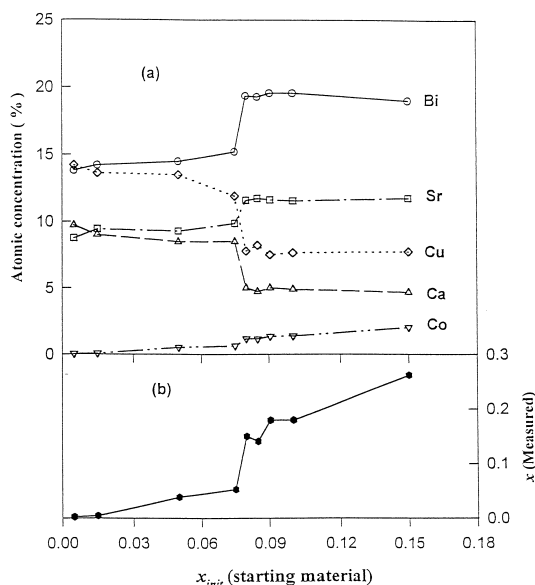


Fig. 1. (a) Atomic composition of the Bi<sub>2</sub>(SrCa)<sub>*n*+1</sub>-(Cu<sub>1-x</sub>Co<sub>*x*</sub>)O<sub>8-δ</sub> whiskers, measured by a non-destructive electron probe microanalysis technique, as a function of the ratio  $x_{\text{init}} = \text{Co}/(\text{Cu} + \text{Co})$  in the starting material. (b) Plot of the measured  $x$  vs.  $x_{\text{init}}$  in the starting material. Lines are a guide to the eye. Note that  $x < x_{\text{init}}$  for  $x_{\text{init}} < 0.08$  but  $x > x_{\text{init}}$  for  $x_{\text{init}} > 0.08$ .

where  $0.25 < x < 0.41$  in their self-flux grown samples. Most individual whiskers were analyzed. The compositions of samples not analyzed were estimated from Fig. 1. We found that the stoichiometry of our whisker remains almost unchanged when the Co concentration is varied, except for the addition of Co, but there is an abrupt jump in stoichiometry at  $x_{\text{init}} \approx 0.08$ . For  $x_{\text{init}} < 0.08$ ,  $x \approx 0.5x_{\text{init}}$ , while for  $x_{\text{init}} > 0.08$ ,  $x \approx 1.8x_{\text{init}}$ . We attribute this concentration jump to a phase boundary between growth of the 2212 phase and the 2201 phase for our whisker samples, as indicated by X-ray diffraction experiments as discussed in Section 2.2. In the region  $x_{\text{init}} < 0.08$ , the fraction of 2223 present decreases, as measured by the resistive jump (see also the bulk measurements below).

### 2.2. Sample characterization with DC, microwave resistance and X-ray diffraction measurements

A standard four-probe DC technique with a typical excitation current  $I = 100 \mu\text{A}$  was used for the

$a$ -axis electric resistance measurements from which we determined  $T_c$ . Electrical contacts were made by evaporating four silver pads on the sample, then annealing at 570°C for 1 min in oxygen flow at 1 atm pressure. Typical contact resistances of roughly 1  $\Omega$  can be obtained when silver paint is applied afterwards.

Fig. 2a shows the typical  $T$  dependence of the normalized resistance along the  $a$ -axis of as-grown (in one atmosphere of oxygen), unsubstituted samples in the range 4 K <  $T$  < 300 K. The resistance is linear in  $T$  in the normal state. The sharp drop in  $R$  at 108 K corresponds to the  $T_c$  of the 2223 phase while the second small drop at about 80 K, shown in the inset of Fig. 2a, corresponds to the  $T_c$  of the

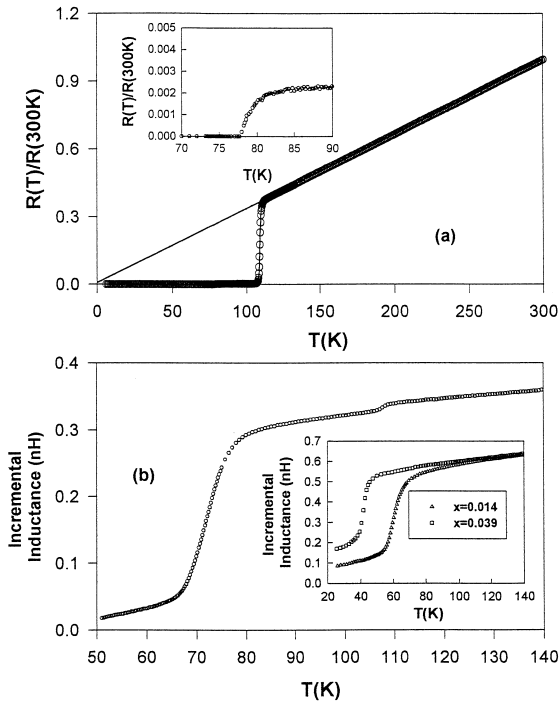


Fig. 2. (a) Normalized DC resistance vs. temperature  $T$  for an unsubstituted whisker. Excellent linearity of the normal-state resistance, a small residual resistance and a narrow transition all reflect the high quality of the whisker samples. The inset shows a blowup plot near the 2212 transition. (b) Microwave inductance measurement. In contrast with the DC measurement, the drop at the 2223 transition is about 20 times smaller than at the 2212 transition. The inset shows that whiskers with higher Co content show essentially no 2223 phase present.

2212 phase. The transition widths (10% to 90%) are  $\sim 1$  K and the transition temperatures are taken at the middle of the transitions in  $R$ . The perfection of these whisker samples leads to a nearly zero extrapolated residual resistance for the unsubstituted samples. Even though the drop in the resistance due to the transition of the 2223 phase is larger than the drop at the 2212 transition for unsubstituted samples, bulk probes, such as X-ray, flux shielding, microprobe analysis and heat capacity measurements, show that the major component in these samples is the 2212 phase, as described in previous work [37].

In order to quantitatively determine the volume fraction of the 2223 phase in our samples, inductive measurements at microwave frequencies were also performed [38]. Each sample was mounted on the cold finger of a two-stage closed-cycle refrigerator. A magnetic field probe, realized by a very small loop antenna at the end of thin coaxial cable, was placed in close proximity to the sample. The other end of the coaxial cable was connected to a Hewlett Packard 8510C microwave vector network analyzer. Throughout the measurement frequency range, the magnetic field probe was very small compared to the excitation wavelength. A physical circuit model consistent with the loop in the proximity of the sample would be quite complex. It would involve the self inductance and resistance of the loop, magnetic coupling to the sample, as well as an equivalent circuit of the sample itself in the transition region. The simplest equivalent circuit for the loop in the presence of the sample consists of an inductor  $L$  and resistor  $R$  in series. Of course,  $L$  and  $R$  are expected to have temperature and frequency dependencies due to the complicated nature of the sample. Since the microwave field in the vicinity of the loop is primarily a reactive magnetic field, nearly all of the incident microwave power is reflected. The phase of the reflected signal, referred to the incident signal, is a measure of the reactive field of the loop. As the sample is cooled through a transition, the magnetic field is expelled from all or part of the sample, perturbing the reactive field of the loop. This is measured as a change in the relative phase of the reflected signal. Although the sample is large compared to the loop, the loop is large compared to the local inhomogeneities caused by the multiple phases (2223 and 2212). Hence, as flux is incrementally

expelled from regions of the sample the measured inductance is changed proportionately. The normal procedure followed is to establish a measurement reference at a temperature above or below the transition region. The sample is then allowed to warm or cool as appropriate. Approximately ten measurements per degree at each of seven discrete frequencies in the 0.05 to 5.0 GHz range can be collected. The microwave reflection coefficient  $S_{11}$  is related to the inductance of the loop probe by:

$$S_{11} = \frac{Z_L - Z_0}{Z_L + Z_0} \quad (1)$$

where  $Z_0$  is the characteristic impedance of the coaxial cable system (50  $\Omega$ ) and  $Z_L$  is the impedance of the loop. The loop, in the presence of the sample, can be modeled as a series combination of an inductor  $L$  and a resistor  $R$ . Then for angular frequencies  $\omega$  such that

$$|R + j\omega L| \ll |Z_0| \quad (2)$$

the magnitude of the  $S_{11}$  is

$$|S_{11}| = 1 - (0.04 \Omega^{-1})R + (0.0008 \Omega^{-1})(\omega L)^2 \quad (3)$$

and the phase angle of  $S_{11}$  is

$$\theta = \pi - (0.04 \Omega^{-1})\omega L [1 + (0.04 \Omega^{-1})R]. \quad (4)$$

Thus,  $\theta$  is not only much more sensitive to a small change in the inductive reactance than is  $|S_{11}|$ , but the change in  $\theta$  is directly proportional to the change in the inductance. Incremental changes in inductance with temperature are proportional to the differential volume from which magnetic flux has been expelled.

As shown in Fig. 2b, drops in  $L$  were observed at 110 and 80 K, corresponding to the 2223 and 2212 phases, respectively. In contrast to DC measurements, the drop in  $L$  at the 2223 phase transition is about 20 times smaller than the 2212 phase, indicating that the volume fraction of the 2223 phase in our samples is approximately 5%.

As mentioned above, the Cu–O planes are parallel to the long axis of the whisker. Flux exclusion measurements [37] and the microwave inductance measurements described above both indicate that the

sample is 2212 with less than 5% inclusion of 2223. Thus, the whiskers can be viewed as a 2212 matrix in which a small volume of 2223 phase, no more than 5%, percolates to form an almost complete filamentary path from one potential contact to the other. Below  $\sim 110$  K, the 2223 phase nearly shorts out the dominant 2212 phase in DC resistance measurements. The only difference between the two phases is an extra Cu–O and Ca–O plane in the 2223 phase. The neighbors of the Co substituent are the same for the two phases in the Cu–O plane and differ in the perpendicular plane only slightly for the middle of the three Cu–O plane. There should be little difference in the chemical potential of Co in the two phases and thus Co should be present equally in the two phases. Further, the experiments indicate that  $dT_c/dx$  is the same for both resistance drops. If Co went into one phase preferentially,  $dT_c/dx$  for that phase would have to compensate by being just the right amount lower so that the observed  $dT_c/dx$  would be equal for the two phases. We believe that to be unlikely, and we therefore assume that the Co substituent enters the two phases with the same fractional substitution.

It is probable that the 2223 exists as laminar, stacking-fault-like laminae parallel to the long dimension of the whisker. Thus, although the 2223 is a minor phase, its ribbon-like occurrence provides a nearly complete superconducting path for  $T$  below the 2223  $T_c$ , but above the 2212  $T_c$ . The presence of 2212 and 2223 conductive paths in the whisker provides an advantageous material venue for the study of doping effects. In a single filamentary crystal sample, which is given a well controlled thermal and oxygenation treatment, the responses of the two superconducting phases to changes in  $x$  in  $\text{Bi}_2(\text{SrCa})_{n+1}(\text{Cu}_{1-x}\text{Co}_x)_n\text{O}_{8-\delta}$  can be determined in a single set of measurements. As  $x$  is increased, the resistive transitions indicate that the fraction of 2223 decreases, although this is a poor measure of the fractional phase content (see Fig. 3a). As shown later, for  $x_{\text{init}} \approx 0.08$ ,  $R$  vs.  $T$  curves appear to show that there are also two phases present. Therefore, X-ray diffraction studies were done to clarify the phase content of the samples with higher Co content.

The X-ray diffraction measurements were performed with a Rigaku AFC7R four-circle diffractometer equipped with graphite-monochromated Mo

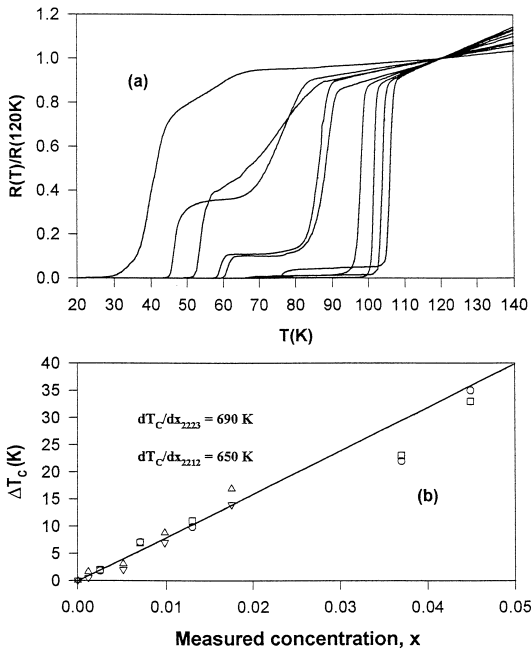


Fig. 3. (a) Normalized resistance (at 120 K) vs.  $T$  for Co-substituted whiskers with  $x_{\text{init}} = 0.005, 0.01, 0.015, 0.05, 0.0375, 0.05, 0.625, 0.075, 0.08$  (from right to left). (b)  $\Delta T_c$  vs. Co concentration for the 2223 (circles) phase and the 2212 (squares) phase. The depression rate  $dT_c/dx$  is determined from a linear least-square fit. A solid line with a slope of  $-800$  K is plotted for reference. The results for a Ni substituted crystal are also presented (up and down triangles for 2212 and 2223 phases, respectively) for comparison.

$K\alpha$  radiation ( $\lambda = 0.71073$ ). Two samples were examined, one with a low Co content ( $x = 0.0044$ ) and one with a high content ( $x = 0.26$ ). The unit cell constants were determined by a least-squares fit of 13 randomly located and centered reflections with a  $2\theta$  range of  $11.4^\circ$ – $24.4^\circ$  for the for Co ( $x = 0.0044$ ) sample. The cell constants are  $a = 0.5378$  nm,  $b = 2.688$  nm,  $c = 3.066$  nm, with  $\alpha = 89.89^\circ$ ,  $\beta = 90.28^\circ$ ,  $\gamma = 89.95^\circ$  and  $V = 0.8864$  nm<sup>3</sup>. The  $b$ -axial rotational photo showed a  $b$  cell constant value of  $1/5$  of 26.88 nm. For the Co ( $x = 0.26$ ) sample, unit cell constants were derived from 14 reflections in a  $2\theta$  range of  $7.8^\circ$ – $25.6^\circ$ . The cell constants,  $a = 0.5371$  nm,  $b = 0.5370$  nm,  $c = 2.417$  nm, with  $\alpha = 89.99^\circ$ ,  $\beta = 90.02^\circ$ ,  $\gamma = 90.01^\circ$  and  $V = 0.6972$  nm<sup>3</sup>, are clearly those of the 2201 phase [39]. Combining X-ray and compositional analysis, we infer that the onset of 2201 occurs for  $x > 0.14$ .

### 3. Results

#### 3.1. Effects of low level Co substitution ( $0 < x \lesssim 0.06$ ) on the superconducting and normal states

Because of the small size of our whiskers, the dimensions of our samples are difficult to determine accurately. Therefore, in Fig. 3a we show the  $T$  dependence of the normalized resistance of Co-substituted samples near the transitions, rather than the resistivity  $\rho(T)$  itself. This also facilitates comparisons between the superconducting behavior of different samples near  $T_c$ . In this figure we plot only those samples that are superconducting. For all these samples we find a linear decrease in  $R$  from 300 K to  $T_c$  (see Fig. 4a) and a dual transition—which we associate with the presence of both the 2212 and 2223 phases. There are several interesting features

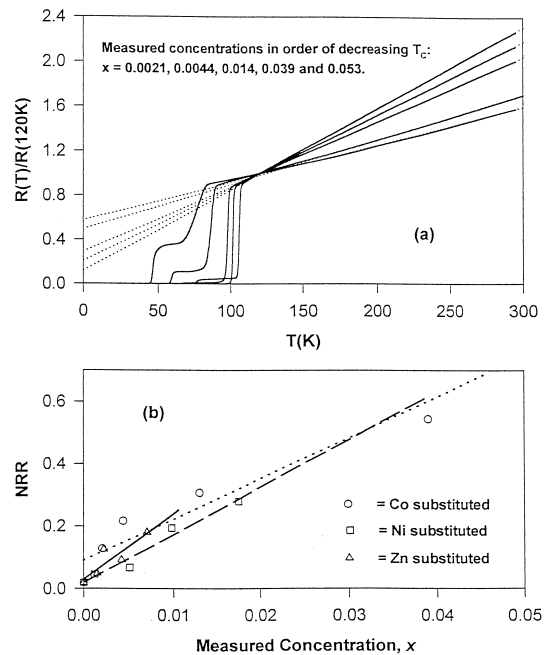


Fig. 4. (a) Same plot as Fig. 3a with an extended temperature range. Fewer samples are shown in this figure for clarity. The normalized residual resistance  $NRR = R(T=0)/R(120\text{ K})$  is defined from a linear fit of the normalized resistance above the 2223 transition extrapolated to  $T = 0$ , shown as dotted straight lines. (b)  $NRR(x) \approx 0.09 + 13x$  for Co, comparable to the values  $NRR(x) \approx 0.02 + 15x$  for Ni and  $NRR(x) \approx 0.03 + 20x$  for Zn which we found in previous work.

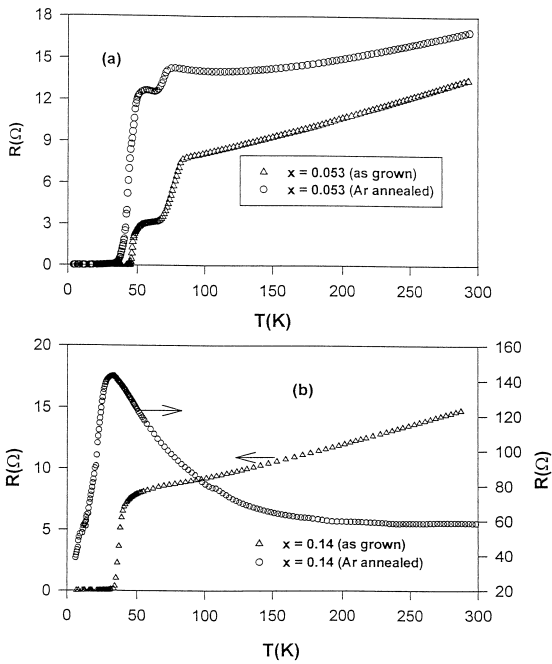


Fig. 5. (a) The DC resistance  $R$  vs.  $T$  for a sample with  $x = 0.053$ . The dependence of  $R$  on  $T$  is very sensitive to oxygenation, with  $dR/dT < 0$  near  $T_c$  under the Ar annealing. (b)  $R$  vs.  $T$  for a sample with  $x = 0.14$ . Ar annealing drives  $dR/dT < 0$  for  $T < 300$  K, but  $\lim_{T \rightarrow 0} R$  apparently goes to zero.

worth mentioning: (i) The fraction of 2223 in the whiskers seems to decrease with increasing  $x$ , as shown in Figs. 3 and 4, although resistance is a poor gauge of phase content. (ii) The  $T_c$ s of both phases decrease monotonically as the amount of Co in the whiskers is increased. From Fig. 3b, we find  $dT_c/dx = -690$  K for Co in the 2223 phase and  $dT_c/dx = -650$  K for the 2212 phase, which are very similar to the values that we found for Ni and Zn substitutions [27]. (iii) The normalized residual resistance  $NRR = R(T=0)/R(120 \text{ K})$ , obtained by extrapolating the normalized normal state resistance to  $T = 0$ , increases with increasing  $x$  as shown in Fig. 4a (fewer samples are shown in this figure for clarity). The NRR increases with increasing  $x$ :  $NRR(x) \approx 0.09 + 13x$  for Co, as plotted in Fig. 4b, comparable to the value  $NRR(x) \approx 0.02 + 15x$  for Ni and  $NRR(x) \approx 0.03 + 20x$  for Zn found in previous work [27]. Since both  $dT_c/dx$  and  $dNRR/dx$  are nearly independent of the substitutional element, we

find that these transition metal substituents influence the superconducting state ( $dT_c/dx$ ) and normal state (NRR) similarly. (iv) A deviation from  $T$  linear resistance toward semiconducting behavior is found for samples with  $x > 0.039$  near  $T_c$ . Some samples with  $x = 0.14$  show zero resistance and some do not (Fig. 5b and Fig. 6). For  $x > 0.14$ , samples no longer have zero resistance and have  $dR/dT < 0$  for some  $T$  (see Fig. 6). Thus,  $x = 0.14$  is a critical concentration. (v) For  $0 < x < 0.14$ ,  $T_c$  for the 2223 phase is only weakly dependent on oxygen concentration, with a maximum for samples annealed in 1 atm of  $O_2$ , for all Co concentrations in this range. The  $T_c$  of the 2212 phase is nearly independent of  $O_2$  annealing (see Fig. 7).

### 3.2. Near the critical concentration: $0.06 < x < 0.18$

In this region, the  $R$ - $T$  curves show a dip (see Fig. 6). The inset to the figure shows that magnetic fields restore the resistance below the dip, which allows us to associate the dip with the presence of a superconducting phase. The temperature of the dip seems to be nearly independent of  $x$ , which is quite

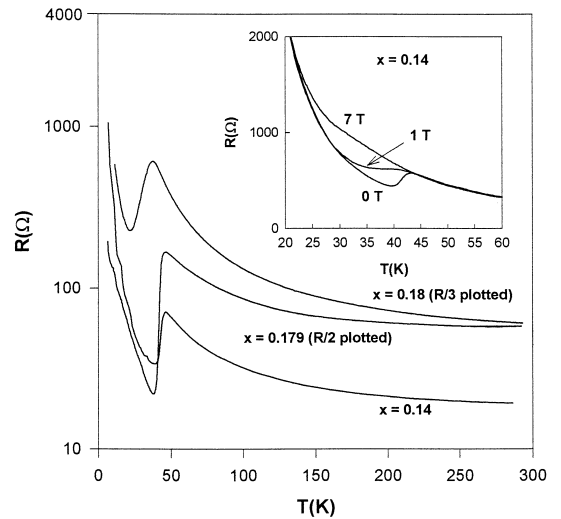


Fig. 6. Variation of  $R$  (note the log scale) with temperature for  $0.14 \leq x \leq 0.18$ . Although  $R$  drops at around 50 K,  $\lim_{T \rightarrow 0} R$  appears to diverge to infinity. Inset: The drop in  $R$  is spread out by an applied field, until at  $\mu_0 H = 7$  T the drop is almost gone. Note that the resistance for the  $x = 0.18$  sample is divided by three and that of the 0.179 sample by two.

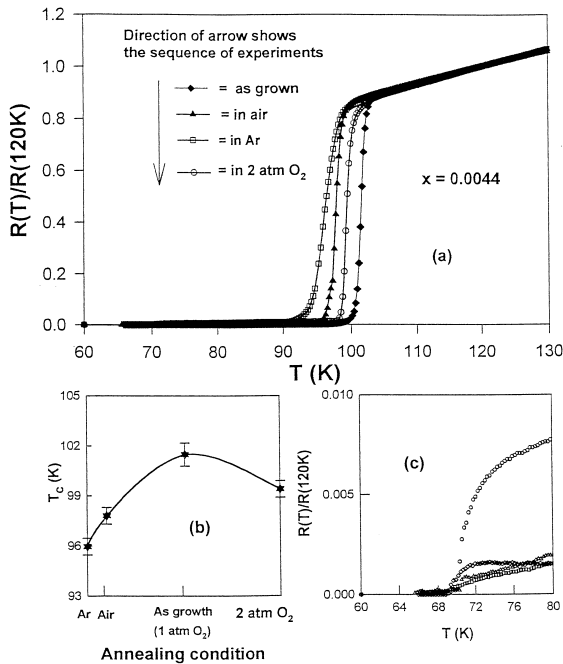


Fig. 7. (a) Normalized DC resistance vs.  $T$  for a sample with  $x = 0.0044$  with oxygen annealing pressure (1 h at  $580^\circ\text{C}$ ) as a parameter. (b) Variation of  $T_c$  (2223) with oxygen content as measured by the  $\text{O}_2$  pressure during the annealing. (c) Within our precision, there is no variation in  $T_c$  (2212) with annealing, symbols as in (a).

different from the behavior for  $x < 0.14$ , and may mean that the maximum  $x$  in the 2212 phase is about 0.14. Near the critical  $x$ , the balance between superconducting and insulating behavior is close, so that it is particularly interesting to see how oxygenation affects this balance. Fig. 5 shows the difference between a sample with  $x = 0.053$  and one with  $x = 0.14$ . Note that these samples were grown from materials that had nearly equal starting material concentrations and that the  $x = 0.053$  sample shows two transitions but the  $x = 0.14$  shows only one. These concentrations lie on either side of the critical concentration shown in Fig. 1b. The onset of the transition in the  $x = 0.14$  sample when Ar annealed is close to the temperature of the onset of the transition in the unannealed sample, which is in turn close to the temperature of the 2212 transition in the  $x = 0.053$  sample. This would argue that the single transition in the  $x = 0.14$  sample is associated with the 2212 phase. Although both Ar annealed samples

show deviations from linearity in the  $R-T$  curves, the Ar annealed  $x = 0.14$  sample has  $dR/dT < 0$  for all  $T > T_c$ .

Fig. 8 shows the behavior of an  $x = 0.14$  Co substituted sample that appears to be just on the edge of the SIT. The as-grown sample has a peak in  $R$  at about 50 K, but  $\lim_{T \rightarrow 0} R = \infty$ . Ar annealing increases  $R$  everywhere, but annealing in 2 atm  $\text{O}_2$  drastically changes the low temperature behavior. The sample evidently goes through the SIT as the  $\text{O}_2$  concentration at the annealing temperature is changed from 1 to 2 atm. Notice that the higher  $\text{O}_2$  concentration lowers the room temperature resistance by nearly an order of magnitude, and makes  $\lim_{T \rightarrow 0} R = 0$ . There is at most a very small range of carrier concentrations for which  $\lim_{T \rightarrow 0} R$  is finite for this  $x = 0.14$  sample. We attribute the dip in  $R$  at about 50 K, which is observed in all annealing conditions for this sample, to the 2212 superconducting transition. The lower temperature transition in this sample annealed in 2 atm  $\text{O}_2$  must then be due to the 2201 phase, which forms the majority of the sample.

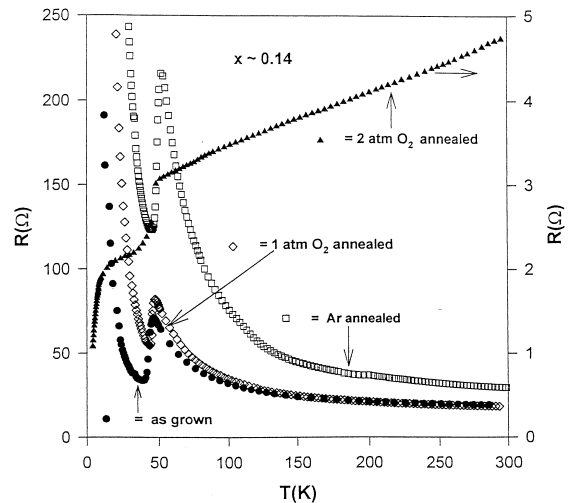


Fig. 8. The  $R$  vs.  $T$  curve for  $x = 0.14$ , with  $\text{O}_2$  annealing pressure as a parameter. The as-grown (in 1 atm  $\text{O}_2$ ) sample has  $dR/dT < 0$  except for a drop in  $R$  near 50 K. Annealing in Ar makes  $dR/dT$  more negative, but annealing in 2 atm  $\text{O}_2$  drives  $dR/dT$  positive everywhere and makes two transitions appear with  $\lim_{T \rightarrow 0} R$  apparently zero. Note the different scale for the 2 atm  $\text{O}_2$  annealed sample. Subsequent annealing in 1 atm  $\text{O}_2$  restores the as-grown behavior.

Thus, this sample shows that Co is a magnetic impurity which does not change  $T_c$  as drastically as it would in a low temperature superconductor (our  $(1/T_c)dT_c/dx = 8$ , as compared to 100 for magnetic Gd in La, 50 for Fe in  $\text{Mo}_{0.8}\text{Re}_{0.2}$  in Sn [40], and 3 for non-magnetic Sb in In [41]), but it can take the sample to the edge of the SIT. Oxygenation allows us to move back and forth across the SIT in a single sample. To our knowledge this is the first time this has been done in BiSCCO. The localization of the carriers is influenced by both the scattering (from Co substitution) and the density of carriers (from oxygenation), but primarily by the former.

At the boundary between the superconducting and insulating states, the zero temperature resistance extrapolated from  $R(T)$  above 100 K is around  $5 \Omega$  for all our samples (see Figs. 5, 6 and 8). The thickness of the samples is about  $5 \mu\text{m}$ , and the distance between double Cu–O planes about 3 nm, so that there are about 1600 double planes in an average sample. The length of an average sample is about 1 mm and the width 0.1 mm, so that there are 10 squares in the measured length. Thus the resistance per square for a single Cu–O plane is about 1.6 k $\Omega$  at the SIT compared to  $h/(2e)^2 \approx 6 \text{ k}\Omega$ , in rough agreement (given the uncertainties in sample dimensions) with the idea that the transition is due to localization [9,15,42,43].

### 3.3. $x > 0.18$

For  $x > 0.18$ , no dip in the resistance is observed (see Fig. 9). As the Co concentration increases  $|dR/dT|$  becomes larger. The temperature dependence is not well fit by semiconducting behavior ( $R = R_0 \exp(-\Delta/T)$ ), but the best fits give  $\Delta \sim 120 \text{ K}$  ( $x = 0.18$ ),  $190 \text{ K}$  ( $x = 0.22$ ) and  $240 \text{ K}$  ( $x = 0.26$ ). Fits to the hopping conduction form  $\rho(T) = \rho_0 \exp(-T_0/T)^\eta$  were attempted (see Fig. 9 inset). The best fit for the  $x = 0.18$  sample is  $\eta = 0.80$ . Different values of the exponent  $\eta$  have been reported by different groups, with  $\eta = 1/4$ ,  $\eta = 1/3$ ,  $\eta = 1/2$ . This sample fits none of these. The best fit  $\eta$  decreases with increasing  $x$ , with  $\eta = 0.62$  for the  $x = 0.22$  sample, and  $\eta = 0.58$  for the  $x = 0.262$  sample. It may be that  $\eta$  is approaching  $1/2$ , implying range hopping is valid for heavily doped samples. Others have also found a doping concentration

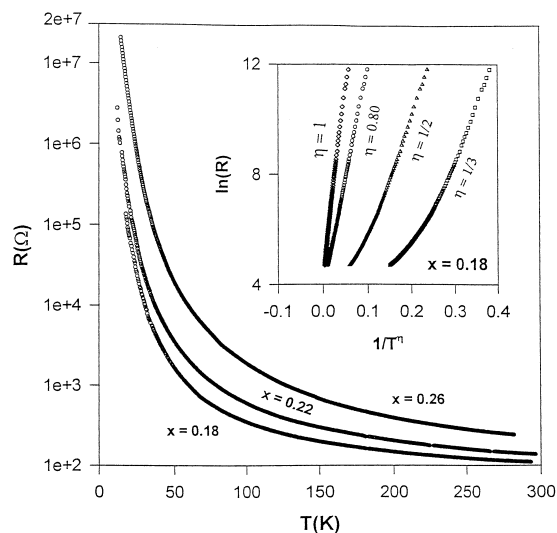


Fig. 9. The  $R$  vs.  $T$  curves for samples with  $x$  greater than 0.18. Fits for  $R = R_0 \exp(T_0/T)^\eta$  for the sample with  $x = 0.18$  are shown in the inset.  $\eta = 0.8$  is the best fit, so that a clear one, two or three-dimensional hopping behavior is not present.

dependent  $\eta$  [11]. The fact that there is no dip in the  $R$  vs.  $T$  curves indicates that the 2212 phase may not be present. These results are consistent with a growth process that yields 2212 for  $x_{\text{init}} < 0.08$  (with an admixture of 2223 that decreases with increasing  $x$ ); mixed 2212 and 2201 for  $0.08 < x_{\text{init}} < 0.10$  and 2201 for  $x_{\text{init}} > 0.10$ . It is interesting to note that the boundary between the 2212 and 2201 phases seems to occur just at the SIT for the 2212 phase.

## 4. Summary

As previously reported [27], our whiskers have the advantage of narrow transitions, easy growth of alloys, and short oxygen annealing times. The short annealing times are due to the small size of the whiskers. Further, this method of growth allowed us to put much more Co in the whiskers than can be put in single crystals grown by traveling solvent or directional solidification techniques, or even ceramic samples. Microprobe compositional analysis shows that the Co went in homogeneously, at least on the scale of the microprobe,  $1 \mu\text{m}^3$ .

We find: (i) a linear depression of  $T_c$  for both the 2212 and 2223 phases with  $dT_c/dx = -700 \text{ K}$ , similar to Ni and Zn substitutions; (ii) a roughly linear increase with  $x$  of the normalized residual

resistance ratio NRR, obtained by extrapolating the normalized resistance (normalized to be unity at 120 K) to  $T = 0$ ; (iii) an SIT occurring at a critical value of  $x \approx 0.06$ ; (iv) that increasing  $x$  reduces the volume fraction of 2223 in our whiskers, and promotes the formation of the 2201 phase for  $x > 0.14$ ; (v) that oxygen doping has only a minor effect at low substitution levels, but a dramatic effect near the critical concentration on both the normal and superconducting properties; and (vi) that localization of carriers through substituent-induced disorder or oxygen-doping lowering of the carrier density is the essential component for the depression of  $T_c$  and for the SIT, rather than pair-breaking.

## 5. Conclusions

Our first conclusion is that, at low concentrations, Co substitution has the same effect as Ni and Zn substitutions for Cu on the electronic properties of BiSCCO. That is, both the normal state resistance and  $dT_c/dx$  are affected in the same quantitative manner by substitution of an equal number of any of these atoms. Thus, both magnetic and non-magnetic substitutions for Cu act like non-magnetic impurities in elemental, s-wave superconductors.

Our second conclusion is that there are two critical concentrations of Co. The first comes as one approaches  $x = 0.06$ , where  $dR/dT$  approaches zero near  $T_c$ . In fact, Fig. 5a shows that an Ar annealed sample with  $x = 0.053$  has a weakly negative  $dR/dT$  near  $T_c$ , implying that localization is about to occur. Oxygenation of samples with  $x_{\text{init}} \approx 0.08$  is particularly interesting. In BiSCCO, the carrier concentration is not very sensitive to oxygenation, and normally one cannot make BiSCCO insulating by oxygen doping. But in a sample that Co substitution has placed just on the border between localized and non-localized carriers, oxygenation can drive the sample back and forth between superconducting and insulating. Thus there are two ways to induce localization: one can limit the mean free path of the carriers and/or one can limit the number of carriers. The second critical concentration is around  $x = 0.18$ . For  $x > 0.18$ , the whiskers no longer show any sign of superconductivity, with  $R \rightarrow \infty$  as  $T \rightarrow 0$ , and appear to be in the 2201 phase. The form of the  $R$

vs.  $T$  behavior is not clearly VRH, but may be approaching the Coulomb-gap VRH form  $R = R_0 \exp(T_0/T)^{1/2}$ .

## Acknowledgements

This work was supported by the Office of Energy Research, Materials Sciences Division, US Department of Energy under contract numbers DE-FG0593ER45493 and DE-FG05-93ER45483. We thank J.J. McGee for assistance with the microprobe analysis, and Roger Eaton for technical assistance.

## References

- [1] Y. Iye, Physical Properties of High Temperature Superconductors III, in: D.M. Ginsberg (Ed.), World Scientific, Singapore, 1992, p. 285.
- [2] Y. Koike, Y. Iwabuchi, S. Hosoya, N. Kobayashi, T. Fukase, Physica C 159 (1989) 105.
- [3] P. Mandal, A. Poddar, B. Ghosh, P. Chaudhury, Phys. Rev. B 43 (1991) 13102.
- [4] N.L. Wang, B. Buschinger, C. Geibel, F. Steglich, Phys. Rev. B 54 (1996) 7445.
- [5] M.Z. Cieplak, S. Gaha, H. Kojima, D. Lindenfeld, G. Xiao, J.Q. Xiao, C.L. Chien, Phys. Rev. B 46 (1992) 5536.
- [6] J.M. Harris, Y.F. Yang, N.P. Ong, Phys. Rev. B 46 (1992) 14293.
- [7] H. Takagai, T. Ido, S. Ishibashi, M. Uota, S. Uchida, Y. Tokara, Phys. Rev. B 40 (1989) 2254.
- [8] C. Kendziora, M.C. Martin, J. Hartje, L. Mihaly, L. Forro, Phys. Rev. B 42 (1993) 3531.
- [9] D.B. Haviland, Y. Liu, A.M. Goldman, Phys. Rev. Lett. 62 (1989) 2180.
- [10] B. Beschoten, S. Sadewasser, G. Guntherodt, C. Quitmann, Phys. Rev. Lett. 77 (1996) 1837.
- [11] C. Quitmann, D. Andrich, C. Jarchow, M. Fleaster, B. Beschoten, G. Guntherodt, V.V. Moshchalkov, G. Mante, R. Manzke, Phys. Rev. B 46 (11) (1992) 813.
- [12] C. Quitmann, P. Almeras, J. Ma, R.J. Kelley, H. Berger, C. Xueya, G. Margaritondo, M. Onellion, Phys. Rev. B 53 (1996) 6819.
- [13] J.M. Valles, A.E. White, K.T. Short, R.C. Dynes, J.P. Garno, A.F.J. Levi, M. Anzlowar, K. Baldwin, Phys. Rev. B 39 (11) (1989) 599.
- [14] P. Almeras, H. Berger, J. Ma, C. Quitmann, M. Onellion, G. Margaritondo, Physica C 235–240 (1994) 957.
- [15] B.G. Orr, H.M. Jaegar, A.M. Goldman, Phys. Rev. B 32 (1985) 7586.
- [16] B. Jayaram, P.C. Laccheester, M.T. Weller, Phys. Rev. B 43 (1991) 10589.

- [17] M.P.A. Fisher, G. Grinstein, S.M. Girvin, *Phys. Rev. Lett.* 64 (1990) 587.
- [18] R. Yoshizaki, Y. Saito, Y. Abe, H. Ikeda, *Physica C* 152 (1988) 408.
- [19] D. Mandrus, L. Forro, C. Kendziora, L. Mihaly, *Phys. Rev. B* 44 (1991) 2418.
- [20] J. Clayhold, S.J. Hagen, N.P. Ong, *Phys. Rev. B* 39 (1989) 7320.
- [21] B. vom Hedt, W. Lisseck, K. Westerholt, H. Bach, *Phys. Rev. B* 49 (1994) 9898.
- [22] S. Doniach, M. Inui, *Phys. Rev. B* 41 (1990) 6668.
- [23] A. Maeda, T. Yabe, S. Takebayashi, M. Hase, K. Uchinokura, *Phys. Rev. B* 41 (1990) 4112.
- [24] M.K. Yu, J.P. Franck, *Phys. Rev. B* 48 (1993) 13939.
- [25] M.K. Yu, J.P. Franck, *Phys. Rev. B* 53 (1996) 8651.
- [26] T. Kluge, Y. Koike, A. Fujiwara, M. Kato, T. Noji, Y. Saito, *Phys. Rev. B* 52 (1995) 727.
- [27] Y.-K. Kuo, C.W. Schneider, M.J. Skove, M.V. Nevitt, G.X. Tessema, J.J. McGee, *Phys. Rev. B* 56 (1997) 6201.
- [28] T. Watanabe, A. Matsuda, *Phys. Rev. B* 54 (1996) 6881.
- [29] M. Boekholt, Th. Bollmeier, L. Buschmann, M. Fleusterand, G. Guntherodt, *Physica C* 198 (1992) 33.
- [30] R.J. Radtke, K. Levin, H.-B. Schüttler, M.R. Norman, *Phys. Rev. B* 48 (1993) 653.
- [31] R.S. Howland, T.H. Geballe, S.S. Ladermann, A. Fisher-Colbrie, M. Scott, J.M. Tarascon, P. Barboux, *Phys. Rev. B* 37 (1989) 9017.
- [32] P.F. Miceli, J.M. Tarascon, L.H. Greene, P. Barboux, F.J. Rotella, J.D. Jorgenson, *Phys. Rev. B* 37 (1988) 5932.
- [33] P. Zolliker, D.E. Cox, J.M. Transguarde, G.S. Shirane, *Phys. Rev. B* 38 (1988) 6575.
- [34] F. Bridges, J.B. Boyce, T. Claeson, T.H. Geballe, J.M. Tarascon, *Phys. Rev. B* 42 (1990) 2137.
- [35] I. Matsubara, H. Tanigawa, T. Ogura, H. Yamashita, M. Kinoshita, T. Kawai, *Jpn. J. Appl. Phys.* 28 (1989) L1358.
- [36] L.W. Lombardo, A. Kapulnik, *J. Cryst. Growth* 92 (1992) 483.
- [37] M. Chung, D.T. Verebelyi, C.W. Schneider, M.V. Nevitt, M.J. Skove, J.E. Payne, M. Marone, P. Kostic, *Physica C* 265 (1996) 301.
- [38] J.M. Pond, L.H. Allen, E.J. Cukauskas, *IEEE Trans. Appl. Supercond.* 7 (2) (1997) 1857–1860.
- [39] R.M. Hazen, *Physical Properties of High Temperature Superconductors*, in: D.M. Ginsberg (Ed.), World Scientific, Singapore, 1990, p. 121.
- [40] B.T. Matthias, *IBM J. Res. Dev.* 6 (1962) 251.
- [41] B.R. Coles, *IBM J. Res. Dev.* 6 (1962) 68.
- [42] T. Pang, *Phys. Rev. Lett.* 62 (1989) 2176.
- [43] D.J.C. Walker, A.P. Mackenzie, J.R. Cooper, *Phys. Rev. B* 51 (1995) 15653.